Cerebral Cortex, November 2020;30: 5639–5653

doi: 10.1093/cercor/bhaa133
Advance Access Publication Date: 9 June 2020
Original Article

ORIGINAL ARTICLE

Overarching Principles and Dimensions of the Functional Organization in the Inferior Parietal Cortex

Gina F. Humphreys, Rebecca L. Jackson and Matthew A. Lambon Ralph

MRC Cognition and Brain Sciences Unit, University of Cambridge, Cambridge CB2 7EF, UK

Address correspondence to Dr Gina Humphreys. Email: gina.humphreys@mrc-cbu.cam.ac.uk; Matt A. Lambon Ralph.
Email: matt.lambon-ralph@mrc-cbu.cam.ac.uk

Abstract

The parietal cortex (PC) is implicated in a confusing myriad of different cognitive processes/tasks. Consequently, understanding the nature and organization of the core underlying neurocomputations is challenging. According to the Parietal Unified Connectivity-biased Computation model, two properties underpin PC function and organization. Firstly, PC is a multidomain, context-dependent buffer of time- and space-varying input, the function of which, over time, becomes sensitive to the statistical temporal/spatial structure of events. Secondly, over and above this core buffering computation, differences in long-range connectivity will generate graded variations in task engagement across subregions. The current study tested these hypotheses using a group independent component analysis technique with two independent functional magnetic resonance imaging datasets (task and resting state data). Three functional organizational principles were revealed: Factor 1, inferior PC was sensitive to the statistical structure of sequences for all stimulus types (pictures, sentences, numbers); Factor 2, a dorsal–ventral variation in generally task-positive versus task-negative (variable) engagement; and Factor 3, an anterior–posterior dimension in inferior PC reflecting different engagement in verbal versus visual tasks, respectively. Together, the data suggest that the core neurocomputation implemented by PC is common across domains, with graded task engagement across regions reflecting variations in the connectivity of task-specific networks that interact with PC.

Key words: angular gyrus, numerical processing, parietal, semantic, sequence processing

Introduction

A long history of neuropsychology and functional neuroimaging has implicated the parietal lobe in a confusing myriad of different cognitive processes and tasks. There is currently little clarity about the underlying core parietal neurocomputations. In a recent large-scale meta-analysis, we investigated the functional organization of the inferior parietal cortex (IPC) across multiple cognitive domains (Humphreys and Lambon Ralph 2015), revealing dorsal–ventral and anterior–posterior organizational graded variations in the types of task that engage IPC. Moreover, each subregion is engaged by multiple diverse tasks indicating that the region is not tessellated into distinct task-specific modules but rather the areas support domain-general computations that are called upon by different activities. Based on these results, we proposed a unifying model of parietal function, the Parietal Unified Connectivity-biased Computation (PUCC). Here, we test some of the central tenants of the model using two independent functional magnetic resonance imaging (fMRI) datasets as well as meta-analytic connectivity modeling.

There are three core assumptions of the PUCC model. The first proposes that the core local computation of the IPC supports online, multimodal buffering. Any time-extended behavior, whether verbal or nonverbal relating to internal or external cognition, requires some kind of internal representation of "the state of play." Without a reliable representation of the current state, it is impossible to check that that the state of the world has changed in the expected manner following the last action, to program the next appropriate steps in the sequence toward the final goal, or to check that the state of the world has not changed dramatically in the interim such that a whole

new goal needs to be instituted. Both automatized and executively guided behaviors require access to an online buffered representation of the "state of affairs." A second key notion relates to the possible broader computational differentiation across ventral (primarily temporal lobe) and dorsal (parietal) pathways. Specifically, the ventral processing routes generalize information across repeated episodes and input modalities, leading to context-independent representations. For example, in the case of semantic memory, multiple instances of a particular exemplar are generalized across time and contexts, thereby allowing it to be recognized in highly variable situations and for information to be generalized across instances and contexts (Lambon Ralph et al. 2010; Buzsaki and Moser 2013; Lambon Ralph 2014). In contrast, the opposite is true for the parietal route, which appears to collapse information across items (i.e., statistically orthogonal to the ventral pathways) extracting item-independent time- and space-varying structures (Buckner and Carroll 2007; Kravitz et al. 2011; Ueno et al. 2011; Bornkessel-Schlesewsky and Schlesewsky 2013). These two proposed features of the IPC—online buffering and extraction of item-independent time-/space-related statistics—can arise from the same computational process. For example, parallel distributed processing (PDP) models have demonstrated that through repeated buffering of sequential input, the system becomes sensitive to the regularities of sequential information (McClelland et al. 1989; Botvinick and Plaut 2004, 2006; Ueno et al. 2011). In the action domain, these statistical structures would support action schema; in the language domain, it might result in the knowledge regarding phoneme or word order (depending on the time resolution over which statistics are computed) as well as number and spatial codings in other domains. A key prediction to be tested in this study was that in such models it is easier to process and buffer sequences that are typical of the domain in question. Accordingly, we would expect activation in IPC to be (a) sensitive to sequential violations and (b) to do so across multiple domains.

There are already hints from past studies that parietal cortex (PC) is sensitive to the temporal structure of events. For instance, IPC has been shown to respond when a word in a sentence is unexpected (Kuperberg et al. 2003; Hoenig and Scheef 2009), when ordering pictures into the correct sequence (Tinaz et al. 2006; Melrose et al. 2008; Tinaz et al. 2008), to scrambled motor sequences compared with learned sequences (Gheysen et al. 2010), to the oddball task (Stevens et al. 2005; Ciaramelli et al. 2008), or to violations in an expected visual sequence (Bubic et al. 2009). Furthermore, the notion that PC buffers context-dependent information is in accordance with several more domain-specific theories. For instance, IPC has been proposed as an "episodic buffer" of multimodal episodic information (Wagner et al. 2005; Vilberg and Rugg 2008; Shimamura 2011), and others suggest that IPC acts as a phonological buffer/sensorimotor interface for speech (Baddeley 2003; Hickok and Poeppel 2007; Rauschecker and Scott 2009). While domain-specific theories have been useful to account for findings from that domain of interest, they fail to explain how and why disparate cognitive domains coalesce in IPC subregions and thus what types of domain-general neurocomputations underlie processing across tasks (Corbetta and Shulman 2002; Humphreys and Lambon Ralph 2015, 2017).

A third assumption in the PUCC model is that, although there might be a common overarching parietal neurocomputation, different parietal subregions show variations in processing based on graded variations in long-range connectivity. Indeed, a large body of work has shown that the IPC shows a reliable response to narratives when the content is intact, compared with narrative stimuli that have been temporally scrambled across multiple domains of input, for example, language or vision (Hasson et al. 2008; Lerner et al. 2011). Previous computational models have demonstrated that, even when the units in the layer of a model have the same core computation, differences in long-range connectivity generate graded variations in emergent function (Plaut 2002). Such connectivity variations might explain differences in the locus of activation in task-based studies (Bzdok et al. 2013; Humphreys and Lambon Ralph 2015). For example, tasks involving tool use have been shown to overlap with numerous other tasks in dorsal PC (top-down attention, executive semantics, phonology, numerical calculation), yet the center of mass of this cluster spreads toward motor and somatosensory areas (Humphreys and Lambon Ralph 2015). Thus, although there may be a high degree of overlap across tasks, the spread of activation for each will vary depending on the task-specific networks that connect to PC.

Such connectivity variations across parietal subdivisions have been demonstrated using structural and functional connectivity measures. Angular gyrus (AG), supramarginal gyrus (SMG), and intraparietal sulcus/superior parietal lobule (IPS/SPL) have been shown to engage partially distinct neural networks: The AG forms part of the default mode network (DMN), the SMG forms part of a cingulo-opercular system, and IPS/SPL is part of a fronto-parietal control system (Vincent et al. 2008; Spreng et al. 2010; Uddin et al. 2010; Cloutman et al. 2013; Power and Petersen 2013). There is some evidence that the transition between regions in terms of their connectivity profile is graded, rather than sharp in nature (Daselaar et al. 2013). Such connectivity-driven variations in function might also explain differences found between anatomically proximate subregions (Uddin et al. 2010; Caspers et al. 2011; Cloutman et al. 2013): Dorsal AG has been found to show positive activation for tasks involving semantic decisions on words and pictures, whereas middle AG is deactivated by both tasks, and ventral AG is activated by pictures but not words (Seghier et al. 2010).

In the current study, three independent datasets and a combination of methods were used to investigate these three core assumptions of the PUCC model. The first method used task-based fMRI. If there is a generalized local buffering computation, then the IPC should activate more for sequential violations. To test this, sequences of items were presented with either a regular structure or one where the structure was violated. Also, the model assumes that, over and above the generalized buffering mechanism, graded task differences will follow from the known variations in connectivity. To test this hypothesis, different types of sequences were presented: comprising words, pictures, or numbers. To test our predictions in more detail, the data were analyzed using a group spatial independent component (ICA). ICA has the advantage of being a data-driven method which can separate signal from noise components associated with movement or physiological fluctuations. As a result, ICA has been shown to possess increased sensitivity compared with standard generalized linear model (GLM) techniques (McKeown et al. 2003). An additional advantage is that ICA can distinguish between distinct components with partial spatial overlap based on variations in time courses (Leech et al. 2011). This point is significant because if subdivisions are graded, we expect some degree of spatial overlap across subregions. Therefore, task ICA was used to investigate the functional networks involved

in processing sequence violations across domains. After establishing the presence of distinct functional PC networks using the task data, an independent resting state dataset was used to independently verify the results.

Methods

fMRI Task Data

Participants

Twenty participants took part in the study (average age = 24.4, standard deviation [SD] = 4.79; # females = 16). All participants were native English speakers with no history of neurological or psychiatric disorders and normal or corrected-to-normal vision.

Task Design

The participants completed three experimental tasks (sentence task, picture task, and number task) in separate scan sessions, the order of which was counterbalanced across subjects. In each task, on a given trial, a sequence of items (words, pictures, or numbers) was visually presented one item at a time with either a familiar structure (normal sequences) or a violated structure in which the final item from each sequence was taken from a different item. The participants' task was to determine if the sequence was coherent. The sequences were selected from the most accurate subset from a pilot experiment. Since this is the first study of its kind to examine sequence violations across the language, pictorial, and number domain using a shared paradigm, we sought to maximize any potential effect by using a highly unexpected sequence ending and an explicit task in which participants were instructed to focus on the coherence of the sequences. An example trial from each task is shown in Figure 1. The items were counterbalanced such that the same participant did not see both the normal or violated versions of the same item.

Sentence task: to ensure a high degree of statistical regularity, sentences were selected in which the final word in the sentence had a high cloze probability and was thus highly predictable (e.g., "He loosened the tie around his neck"). The stimuli were a subset of the high cloze probability items included in Block and Baldwin (2010) (average cloze probability = 0.94, SD = 0.01). The sentence length varied from 6 to 10 words (average length = 8.4 words, SD = 1.0).

Picture task: a series of four color pictures depicted the occurrence of real-life, everyday events with a clear causal structure, that is, the events could not plausibly occur in a different order (e.g., a banana being peeled, a house being built, etc.). The images consisted of stills taken from freely available short online video clips downloaded from youtube.com. In each case, the event of interest was the central focus of the videos, and there was minimal distracting background information.

Number task: a series of four numbers involving low-digit multiplication (e.g., 2 4 6 8) or addition (e.g., 1 2 3 4). Low-digit multiplication and addition have been shown to be automated skills, the solutions to which can be easily retrieved from memory (Simon et al. 2002; Dehaene et al. 2003). Note that the high accuracy scores for the task (see Results section) confirm that the sequences were easily recognizable.

Task Procedures

There were 42 items per condition presented using an event-related design with the most efficient ordering of events determined using Optseq (http://www.freesurfer. net/optseq). Null time was intermixed between trials and varied between 2 and 18 s (average = 4.59 s, SD = 3.06) during which a fixation cross was presented. For the picture and number task, each of the four items in the sequence was presented for 900 ms (total length = 3.6 s). The word sequences in the sentence task contained between 6 and 10 words presented at a rate of one word every 360 ms such that the maximum trial duration matched the picture and number task. Every item was followed by a "?" for 1.4 s at which point the participants provided a YES/NO button response.

Task Acquisition Parameters

Images were acquired using a 3 T Philips Achieva scanner using a dual gradient-echo sequence, which is known to have improved signal relative to conventional techniques, especially in areas associated with signal loss (Halai et al. 2014). Thirty-one axial slices were collected using a TR = 2.8 seconds, TE = 12 and 35 ms, flip angle = 95°, 80 × 79 matrix, with resolution 3 × 3 mm, slice thickness 4 mm. Across all tasks, 918 volumes were acquired in total, collected in 6 runs of 428.4 s each. B0 images were also acquired to correct for image distortion.

Task Data Analysis

Preprocessing

The dual-echo images were first B0 corrected and then averaged. Data were analyzed using SPM8. After motion correction images were coregistered to the participants T1. Spatial normalization into MNI space was computed using DARTEL (Ashburner 2007), and the functional images were resampled to a 3 × 3 × 3 mm voxel size and smoothed with an 8-mm full-width at half maximum (FWHM) Gaussian kernel.

General Linear Modeling

The data were filtered using a high-pass filter with a cutoff of 190 s and then analyzed using a GLM. At the individual subject level, each condition for each task was modeled with a separate regressor (normal, violated) with time and dispersion derivatives added, and events were convolved with the canonical hemodynamic response function. Each sequence was modeled as a single event. Motion parameters were entered into the model as covariates of no interest. To investigate the effect of violation, the contrast of violation sequences > normal sequences was computed in a whole-brain analysis (uncorrected, $P < 0.001$), with a significant cluster extent estimated using AlphaSim with $\alpha < 0.05$ and a brain mask applied (https://afni.nimh.nih.gov/pub/dist/doc/program_help/AlphaSim.html). More targeted analyses were also conducted using the parameter estimates. Both GLM and ICA methods have advantages and disadvantages, and thus we performed both here. While GLM is a highly informative fMRI analytic approach, ICA has been shown to reveal a wider task-related network compared with GLM analyses (Robinson et al. 2013), as well as the potential to show distinct yet spatially overlapping functional networks (Xu et al. 2013, 2016). On the other hand, GLM has other advantages including the ability to explore BOLD time courses across longer trials than those used in the current study (e.g., van der Linden et al. 2017).

Task Group Spatial ICA

The preprocessed fMRI data were analyzed in a group spatial ICA using the GIFT toolbox (http://mialab.mrn.org/software/gift) (Calhoun et al. 2001) to decompose the data into its components,

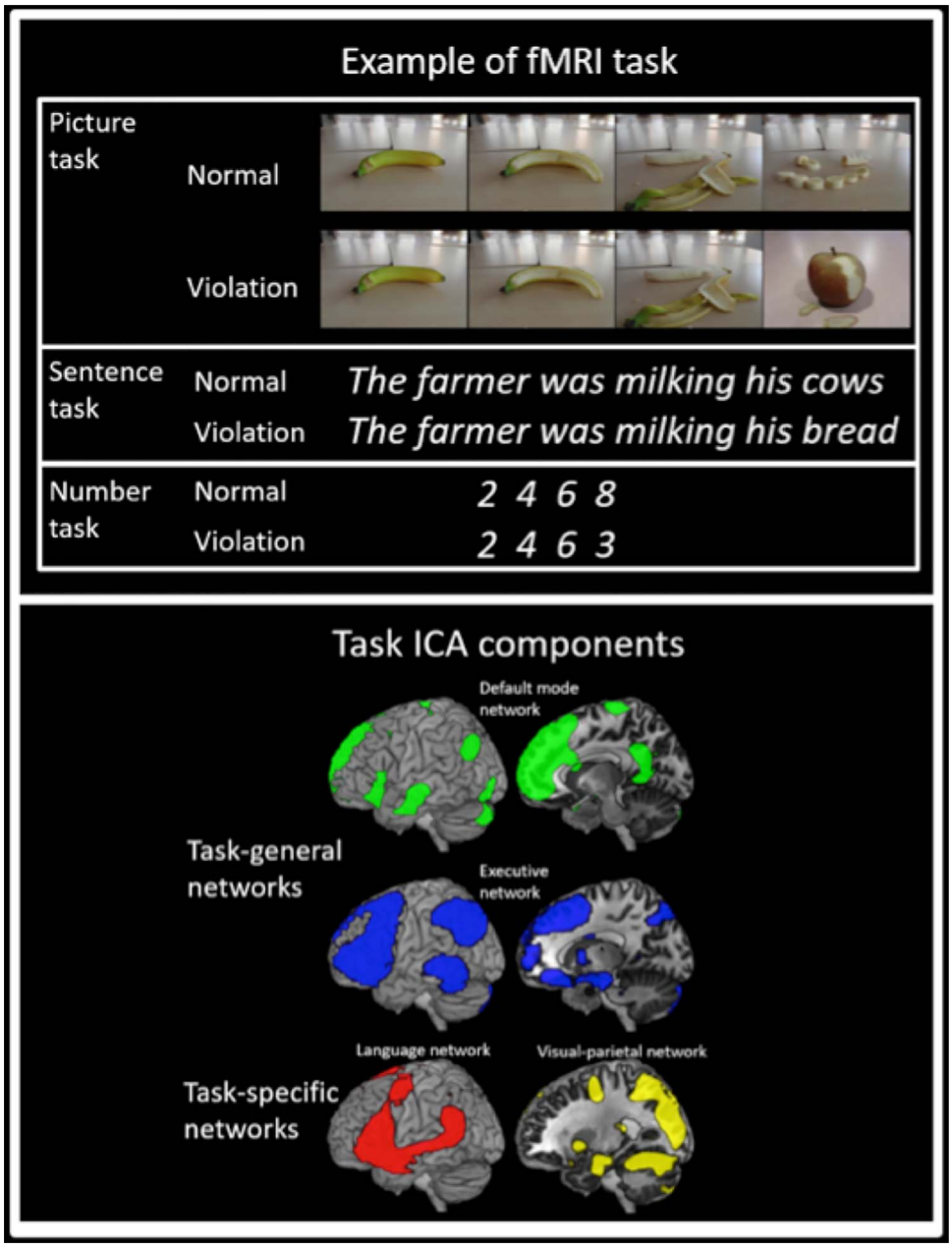

Figure 1. Top panel: An example from one trial for each of the tasks. Bottom panel: The task-general and task-specific ICA components (cluster corrected, $P < 0.05$).

separately for each task. GIFT was used to concatenate the subjects' data and reduce the aggregated dataset to the estimated number of dimensions using PCA, followed by an ICA analysis using the infomax algorithm (Bell and Sejnowski 1995). There were found to be nine non-noise components for the number task, 11 for the picture task, and 13 for the sentence task. One-sample *t*-tests were used to identify areas that significantly contributed to each component (cluster corrected, $P < 0.05$). The thresholded *t*-maps were then inspected, and verbal labels were assigned to each network, where possible labels were used which were consistent with those used frequently elsewhere in the literature (e.g., DMN, motor network, visual network, language network, saliency network) (Power et al. 2011; Lee et al. 2012; Yeo et al. 2013).

Certain components were found to be common to all tasks (see Supplementary Material, Fig. S1), we shall therefore refer to these as task-general networks. We defined task-general networks based on the degree of spatial overlap across components (all comparisons had a Dice coefficient > 0.7, which is considered a high degree of spatial overlap). These closely resemble those that are commonly labeled as a DMN component and a fronto-parietal executive control component (described in detail in Results section). An additional network resembling that commonly referred to as the saliency network was also present which included the temporo-parietal junction (TPJ); however this component was found to be insensitive to any task manipulation and was therefore not included in further analyses (no task modulated TPJ activation relative to rest

[all ts < 1.3, ps > 0.2], nor was there any modulation based on violation [all ts < 1.4, ps > 0.2]). We have now measured this was similarly the case for the executive network components (Dice coefficient > 0.7 in all pair-wise comparisons).

In addition to the task-general components, we also identified two task-specific left parietal components (i.e., components which were not common to each task); a network that we have labeled as the "language component" from the sentence task and a "visual-parietal component" from the picture task (described in detail in Results section).

In order to interrogate the cognitive signature of each component, 12-mm spheres were defined around the peak coordinates from all components of interest, and these were used as regions of interest (ROIs) to test for significant effects of conditions. Finally, we also examined how parietal networks might interact with one another or with other networks in the brain (e.g., visual or auditory) by performing a crosscorrelation analysis of the average time-series for these components (parietal or nonparietal).

Resting State Data

Participants, Procedures, and Acquisition Parameters

Seventy-eight participants completed the resting state scan (average age = 25.23, SD = 5.55; # females = 57). During the scan, the participants were instructed to keep their eyes open and look at the fixation cross. The data acquisition parameters for the resting state scan were identical to the experimental task. The scan consisted of a single 364-s scan session of 130 volumes.

Data Analysis

Preprocessing: Preprocessing was performed using SPM8 and the Data Processing Assistant for Resting State fMRI (DPARSF Advanced Edition, V2.3) toolbox (Chao-Gan and Yu-Feng 2010). Compared with the task data, additional preprocessing steps were carried out on the resting state data to minimize the influence of distance-dependent increases in correlations due to motion, which are considered problematic in resting state data. Thus, several procedures were adopted: censoring, global signal regression, 24 motion parameter regression, and scrubbing of high motion time points. These methods have been shown to greatly reduce the effects of motion (Weissenbacher et al. 2009; Van Dijk et al. 2012; Yan et al. 2013; Power et al. 2014).

The images were first slice-time corrected, realigned, and coregistered to the subjects T1 using SPM. Censoring was applied using a threshold of greater than 3 mm of translation or 1 degree of rotation. This resulted in the exclusion of six participants from further analysis. Using DPARSF, images were normalized using DARTEL, smoothed with a 8-mm FWHM Gaussian kernel, and filtered at 0.01–0.08 Hz (Satterthwaite et al. 2013). Nuisance covariates were regressed out. These included covariates for 24 motion parameters, white matter, CSF, and global tissue signal and also the performance of linear detrending. The 24 motion parameters were calculated from the six original motion parameters using Volterra expansion (Friston et al. 1996) and have been shown to improve motion correction compared with the six parameters alone (Yan et al. 2013; Power et al. 2014). Additional covariates were included for outlier time points with a with a z-score >2.5 from the mean global power or >1-mm translation as identified using the ARtifact detection Tools software package (ART; www.nitrc.org/projects/artifact_detect).

Resting state ICA: The goal of the resting state ICA analysis was to use an independent dataset to verify the AG functional subdivisions identified by the task ICA. The ICA was carried out on the preprocessed resting state data using the same method as the task data. This analysis identified five AG components, the significance of which was tested using one-sample *t*-tests (cluster corrected, $P < 0.05$). These five AG subdivisions were then used as ROIs for the task data to test for effects of violation and task. The spatial similarity of the parietal ROIs defined using the task ICA versus the resting state ICA and observed Dice coefficients varying from 0.2 to 0.6 (dorsal PGa = 0.4, mid-PGp = 0.4, ventral PGa = 0.6, and ventral PGp = 0.2). This is a good level of overlap when considering that the components were identified using different fMRI techniques (resting state vs. task fMRI) and using different subjects.

Results

Behavioral Results

Task performance was highly accurate across all experimental tasks (sentence task = 97%, SD = 3.3; picture task = 93%, SD = 5.8; number task = 91%, SD = 8.1). Nevertheless, there were some task differences: The sentence task was found to be significantly more accurate than the number task ($t(19) = 3.17$, $P = 0.005$, $d = 0.71$) and marginally more accurate than the picture task ($t(19) = 2.52$, $P = 0.02$, $d = 0.71$), which does not survive Bonferroni correction. The picture task was marginally more accurate than the number task ($t(19) = 2.17$, $P = 0.04$, $d = 0.49$), which does not survive Bonferroni correction.

In terms of reaction time, a 3 × 2 within-subjects ANOVA found a significant effect of task ($F(38) = 18.13$, $P = 0.001$, $\eta p^2 = 0.49$), violation ($F(38) = 7.71$, $P = 0.01$, $\eta p^2 = 0.29$) and a significant task × violation interaction ($F(38) = 22.09$, $P = 0.001$, $\eta p^2 = 0.54$). Paired *t*-tests showed that responses to the sentence task were slower compared with the picture task ($t(19) = 6.35$, $P = 0.001$, $d > 1.75$) and the number task ($t(19) = 5.35$, $P = 0.001$, $d = 1.36$) which did not differ ($t(19) = 1.06$, $P = 0.30$). The interaction can be explained by an effect of violation in the picture task ($t(19) = 5.75$, $P = 0.001$, $d = 1.28$), but no significant difference for the sentence task or number task (all ts < 2 ps > 0.05).

GLM Analysis

Compared with the normal sequences, the violation sequences elicited greater activation within IPC for all tasks (see Supplementary Material, Fig. S2 and Table S1), with overlap in medial posterior AG (PGp). There was some overlap in the violation > normal contrast in the DLPFC, although this cluster did not survive the cluster correction for the number task. No parietal voxels showed the opposite pattern (normal > violation), even at a very lenient threshold (all ts < 1). Some task differences were found to be significant. The violation effect was found to be significantly larger for the sentence task compared with the other two tasks combined (Sentences > Pictures + Numbers) in the anterior AG (PGa), left lateral frontal areas (inferior frontal gyrus [IFG] and precentral gyrus), and right superior temporal gyrus. The left posterior middle temporal gyrus was also more strongly recruited for the sentence task; however, this did not survive the cluster correction. The violation effect for the picture task was found to be greater than the sentence and number tasks combined (Pictures > Sentences + Numbers) in a network of bilateral visual areas (fusiform gyrus and visual cortex). There were no regions more responsive to the number task compared with the other two tasks. Therefore, these analyses support

the hypothesis that IPC, especially AG, is sensitive to sequence violations but also suggests that there may be task differences in the full network recruited.

Task ICA Analysis

Task-General Networks

Certain parietal components were found to be largely overlapping across tasks (task-general networks). These resemble a DMN component (bilateral posterior AG, precuneus [PCC], medial frontal, mid-middle temporal gyrus [MTG]), a fronto-parietal executive control component (referred to as the executive network from here on, including left lateral frontal, AG/IPS, pMTG, and posterior superior frontal gyrus [SFG]). The DMN and executive control network overlapped in AG; however the peak for the executive control network was found to be more dorsal, approaching IPS. Both networks also overlapped in IFG and SFG, although the peak activation was more dorsal for the executive control network (Fig. 1).

There were two parietal components that were task-specific in nature (see Fig. 1). First, there was a visual–parietal network that involved visual cortex, SPL, and PGp, which was present in the picture task alone. Second, there was a component identified from the sentence task data that clearly resembled what is often referred to as the language network (left IFG, MTG, anterior AG) (Vigneau et al. 2006).

Sensitivity of task-general and task-specific networks to violation. In order to examine the cognitive signatures of each identified component, spheres were defined around the peak coordinates from the task-general (DMN, executive network, and saliency network) and task-specific networks (language, visual–parietal, and IPS number), and these were used as ROIs to test for effects of violation.

Task-General Parietal ROIs

The AG ROI for the executive network was more dorsal (in PGa, here on referred to as dorsal PGa) compared with the DMN ROI, which was in central AG (in PGp) (here on referred to as mid-PGp). Both ROIs showed an overall effect of violation, which did not interact with task: Within the DMN, mid-PGp showed a significant effect of violation ($F(1,19) = 5.73$, $P = 0.03$, $\eta p^2 = 0.23$) but no effect of task ($F(2,38) = 1.75$, $P = 0.19$) and no task x violation interaction ($F(2,38) = 0.01$, $P = 0.99$). Within the executive network, the dorsal PGa ROI showed a significant effect of violation ($F(1,19) = 18.63$, $P = 0.001$, $\eta p^2 = 0.55$), a marginal effect of task ($F(2,38) = 3.01$, $P = 0.06$, $\eta p^2 = 0.14$), but no task x violation interaction ($F(2,38) = 1.96$, $P = 0.16$). The effect of task reflected moderately stronger activity for the picture compared with number tasks; however, this did not survive a Bonferroni correction ($t(19) = 2.23$, $P = 0.04$).

Despite the AG components of the executive network and DMN showing similar task-general sensitivity to sequence violations, the two subregions exhibited opposing directions of activation relative to fixation; activation for the executive network was significantly greater than zero for each condition (one-sample *t*-test, all $ts > 3.49$, $ps < 0.002$, $ds > 0.78$), whereas the DMN elicits significant negative activation for each condition (one-sample t-test, all $ts > -3.68$, $ps < 0.002$, $ds > 1.01$, although the sentence violation condition only trended after Bonferroni correction was applied ($t(19) = -2.8$, $P = 0.01$, $d = 0.6$). This suggests that while both areas show a similar effect of violation, the underpinning function of each subdivision is likely to differ, perhaps reflecting the fact that the dorsal PGa is part of the task-positive executive network, whereas the mid-PGp is part of the DMN which often shows a task-negative response. These results from all regions are presented in Figure 2 (and see Supplementary Material, Fig. S3 for an alternative view of the ROIs).

Task-General Nonparietal ROIs

Given that the AG component of the executive and DMN were both sensitive to sequence violations, further analyses were conducted on the nonparietal components of the networks so as to determine whether the effect was AG-specific or general to the whole of the network (see Fig. 3).

Within the DMN, no other region was found to be sensitive to violation. There were no significant effects for ventral IFG or PCC (all $Fs < 2.58$, $ps > 0.13$). Mid-MTG and medial frontal showed a significant effect of task but no effect of violation and no interaction (mid-MTG, task $F(2,38) = 18.95$, $P = 0.001$, $\eta p^2 = 0.55$, condition $F(1,19) = 0.30$, $P = 0.59$, interaction $F(2,38) = 0.47$, $P = 0.63$; Medial frontal task, $F(2,38) = 5.35$, $P = 0.009$, $\eta p^2 = 0.22$, condition $F(1,19) = 0.08$, $P = 0.78$, interaction $F(2,38) = 0.85$, $P = 0.44$). For mid-MTG, sentences elicited greater activity compared with pictures ($t(19) = 5.45$, $P = 0.001$, $d = 1.22$) and numbers ($t(19) = 4.28$, $P = 0.001$, $d = 0.96$), which did not differ ($t(19) = 1.58$, $P = 0.13$). Within the medial frontal ROI, numbers elicited greater activity compared with pictures ($t(19) = 3.52$, $P = 0.002$, $d = 1.01$). Therefore, the AG is the only DMN area to respond to sequence violations.

Unlike the DMN, all regions of the executive network showed task-general sensitivity to violation, with stronger activation for the violation condition compared with the normal sequences. Within the dorsal IFG, there was a significant effect of task ($F(2,38) = 6.27$, $P = 0.004$, $\eta p^2 = 0.25$), violation ($F(1,19) = 14.60$, $P = 0.001$, $\eta p^2 = 0.44$), but no significant task × violation interaction ($F(2,38) = 0.20$, $P = 0.82$). The task effect reflects greater activity for sentences compared with numbers ($t(19) = 3.10$, $P = 0.006$, $d = 0.69$) and pictures ($t(19) = 2.46$, $P = 0.02$, $d = 0.55$). Similarly, within posterior MTG there was a significant effect of task ($F(2,38) = 18.11$, $P = 0.001$) and violation ($F(1,19) = 13.55$, $P = 0.002$) and no significant task × violation interaction ($F(2,38) = 2.54$, $P = 0.09$). The task effect reflected reduced for numbers compared with pictures ($t(19) = 5.74$, $P = 0.001$, $d = 1.28$) and sentences ($t(19) = 4.56$, $P = 0.001$, $d = 1.01$).

Task-Specific Parietal ROIs

Language network: The anterior ventral AG (here on referred to as ventral PGa) showed a significant effect of task ($F(2,38) = 26.92$, $P = 0.001$, $\eta p^2 = 0.59$), violation ($F(1,19) = 10.75$, $P = 0.004$, $\eta p^2 = 0.39$), and a significant task × condition interaction ($F(2,38) = 5.93$, $P = 0.006$, $\eta p^2 = 0.24$). The task effect reflects stronger activation for the sentence task compared with the picture task ($t(19) = 6.15$, $P = 0.001$, $d = 1.37$) and the number task ($t(19) = 7.32$, $P = 0.001$, $d = 1.64$). The interaction can be explained by a stronger effect of violation in the sentence task compared with the picture task ($t(19) = 3.12$, $P = 0.006$, $d = 0.70$) and the number task ($t(19) = 2.92$, $P = 0.009$, $d = 0.65$). One-sample *t*-tests were used to examine whether the activation differed significantly from zero and if so in which direction. This showed significantly positive activation for the sentence conditions only ($ts > 4.72$, $ps < 0.001$, $d = 1.01$), with the picture and number conditions showing no difference from zero ($ts < 0.92$, $ps > 0.37$). Therefore, while this area is sensitive to violation overall, the effect is larger in the sentence task, which is also the only task to positively activate this region. This difference is likely explained by the fact that this region forms

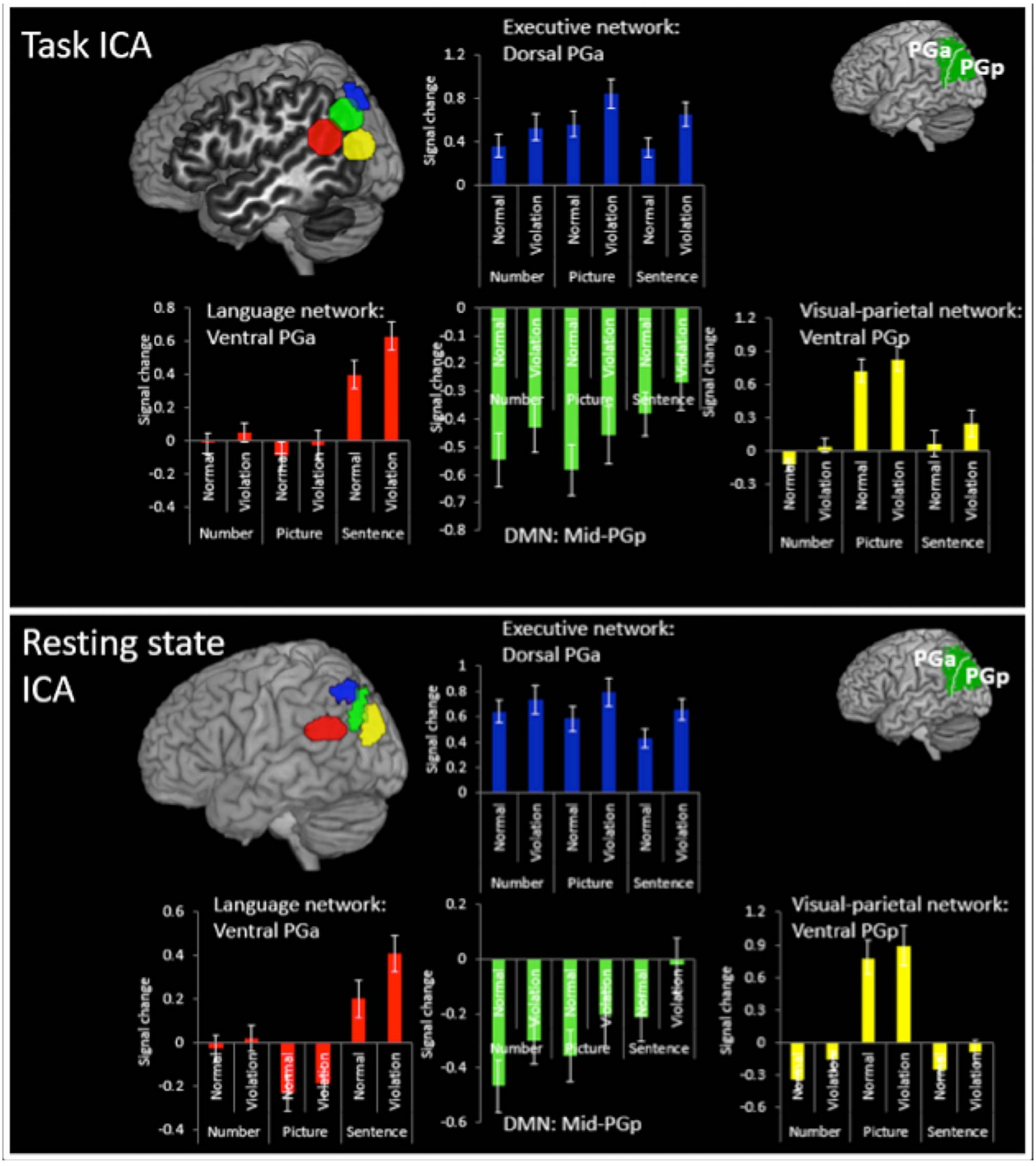

Figure 2. Percent signal change for the violation and normal sequences for each task within the task ICA ROIs and resting state ICA ROIs. The results show the same pattern for both methods.

part of the language network and hence responds strongly to linguistic stimuli. These results are presented in Figure 2 (see Supplementary Material, Fig. S3 for an alternative anatomical view of the ROIs).

Visual–parietal network: The posterior ventral AG (here on referred to as ventral PGp) was specifically sensitive to the picture task. The results showed a significant effect of task ($F(2,38) = 50.86$, $P = 0.001$, $\eta p^2 = 0.73$), violation ($F(1,19) = 23.69$, $P = 0.001$, $\eta p^2 = 0.56$), but no task × violation interaction ($F(2,38) = 1.16$, $P = 0.33$). The picture task elicited stronger activation than the number task ($t(19) = 10.02$, $P = 0.001$, $d = 2.24$) and the sentence task ($t(19) = 7.62$, $P = 0.001$, $d = 1.70$), which differed marginally in favor of the sentence task after applying Bonferroni correction ($t(19) = 2.20$, $P = 0.04$, $d = 0.02$). Examinations of the direction

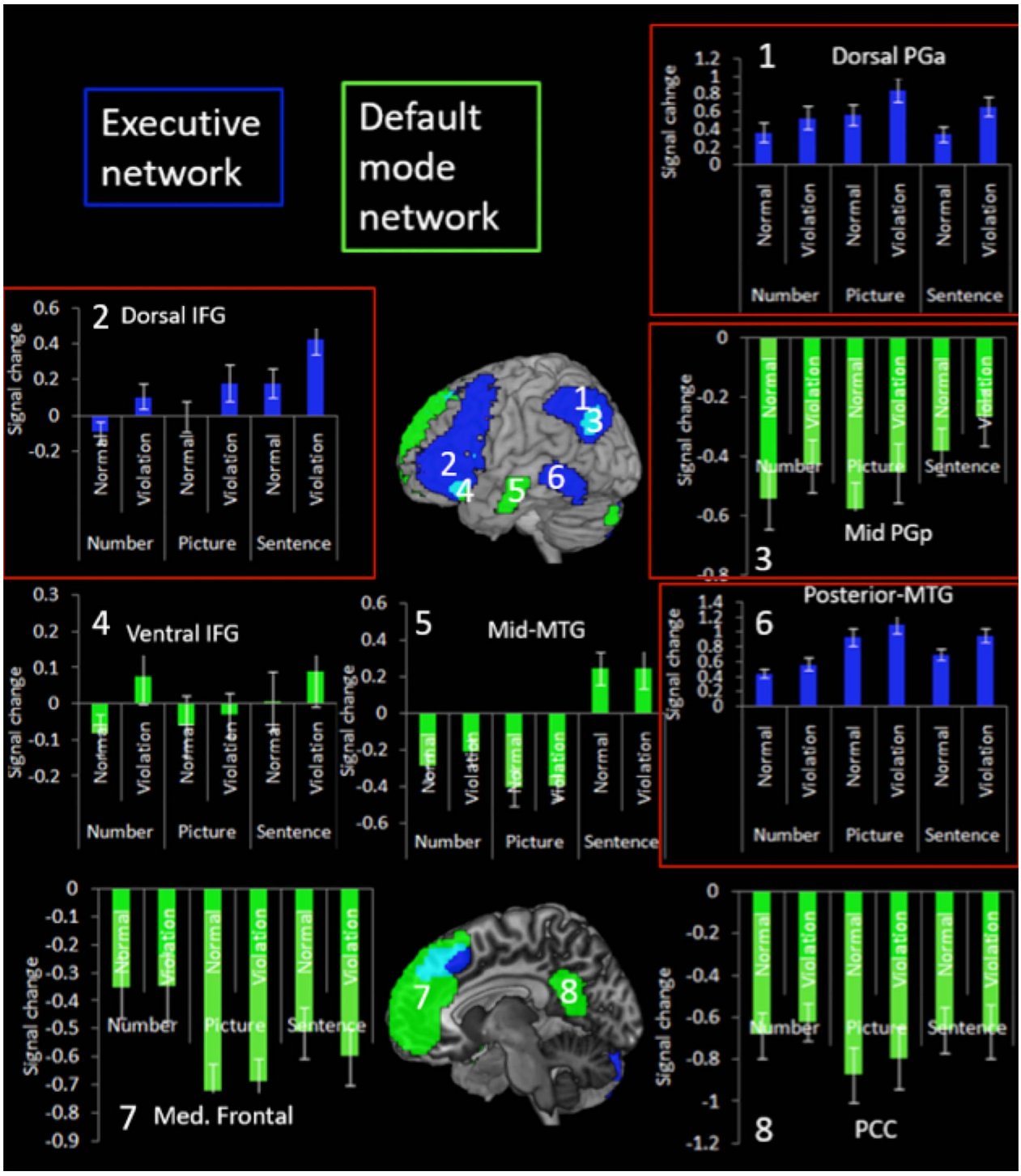

Figure 3. Percent signal change for the violation and normal sequences for each task within the executive network and default mode network. The regions to show a significant effect of violation are highlighted in red.

of activation revealed significantly positive activation for the picture task only ($ts > 6.35$, $ps < 0.001$, $d = 1.42$), with no modulation of the sentence and number tasks ($ts < 2$, $ps > 0.05$). Therefore, while this area is sensitive to violation overall, it shows a task-specific response to picture task likely due to the fact that this region is part of a visual processing network. These results are presented in Figure 2 (see Supplementary Material, Fig. S3 for an alternative anatomical view of the ROIs).

Crosscorrelations

We examined how parietal networks might functionally relate to one another and also to the nonparietal neural networks by

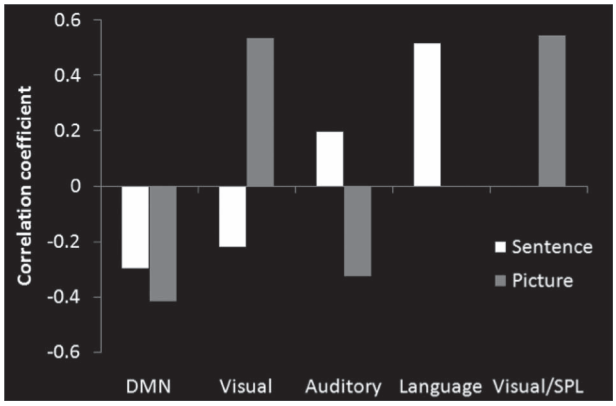

Figure 4. The crosscorrelation with the average time course of the executive network.

measuring the crosscorrelations between each network's time-series (Bonferroni corrected). Besides the networks mentioned above, we additionally included in this analysis the task-general auditory (bilateral auditory cortex) and visual networks (bilateral visual cortex) in order to have a common comparison across tasks and test whether each task differentially engaged each modality (e.g., picture tasks might correlate more strongly with visual components). Interestingly, like in the analyses described above, there was a dissociation in responses for the picture task compared with the sentence task (Fig. 4). These showed a strong anticorrelation between the executive network (and related networks) and the DMN for both tasks, thus suggesting that activation of the executive network may relate to suppression in the DMN.

For the sentence tasks, the executive network showed a significant positive correlation with the language network and also the auditory network (even though the sentences were visually presented) ($r = 0.52$, $r = 0.20$, respectively, ps < 0.01), but a negative correlation with visual networks and DMN ($r = -0.22$, $r = -0.30$, respectively, ps < 0.001). Whereas, in the picture task, the executive network instead correlated positively with visual networks (rs $= 0.54$, ps < 0.001) and negatively with auditory networks and DMN ($r = -0.34$, $r = -0.42$, respectively, ps < 0.001). This suggests that while the executive network is task-general, there is a shift in the networks that interact with it based on the varying demands of each task. Furthermore, when a network is not required for that particular task, it becomes anticorrelated with the executive network. (Note, we dropped the number task from this analysis because a "number network" is not well established in the literature. Without a well-established network to identify, it is not clear how to select a "number ICA component" for use in the crosscorrelation analysis. In contrast, visual and auditory components are well established and could be easily identified.)

Summary

The task ICA results suggest that IPC as a whole is sensitive to sequence violations. However, IPC subregions appear to be organized along dorsal–ventral and anterior–posterior dimensions. Specifically, dorsal PGa and mid-PGp showed task-general responses, yet the time-series of the two networks were anticorrelated and the subregions had opposing activation directions relative to rest: Dorsal PGa was positively activated by all tasks, whereas ventral mid-PGp was deactivated.

Whereas these areas showed a task-general response to violation, anterior and posterior portions of ventral IPC showed task-specific responses. Specifically, ventral PGa was only positively activated by sentence tasks, whereas ventral PGp responded positively to picture tasks alone. This pattern mirrors the variations in the networks that correlate with each subregion. Specifically, ventral PGa is part of the language network and hence is positively activated for sentence tasks, whereas ventral PGp is part of a visual network and hence responds to picture tasks. There was also a dynamic, task-specific switching between the executive network and the other networks; for the sentence, task the executive network correlated with language and auditory networks and was anticorrelated with visual areas, but for the picture tasks the opposite pattern was found.

Resting State ICA

The resting state ICA analysis was used to verify the presence of the functional subdivisions using an independent dataset and in the absence of a task. This ICA revealed five components which involved IPC. Components 1 and 2 engaged partially overlapping regions of dorsal PGa. Component 1 included a similar network as the executive component from the task ICA analysis (lateral frontal, dorsal PGa, and pMTG), while component 2 was more restricted in size but still recruited lateral frontal and dorsal PGa. Component 3 engaged mid-PGp region and was similar to the DMN identified in the task ICA analysis. Component 4 engaged ventral PGa and resembled the language network from the previous analysis. Finally, component 5 engaged ventral PGp and included a network of superior parietal and higher-level visual areas which included some of the same regions as the visual/SPL network from the task ICA analyses. Thus, there appeared to be strong correspondence between the networks identified in the task-based and resting state ICA analyses (see Fig. 5).

The five rs-fMRI–derived IPC subdivisions were used as ROIs for the task data to examine whether they showed a similar pattern of sensitivity to violation across tasks as those regions defined by the task ICA (see Fig. 2; Supplementary Material, Fig. S3). Responses within components 1 and 2 were found to be similar to the dorsal PGa region from executive network in the task ICA data. Both components 1 and 2 showed a significant effect of violation (component 1, $F(1,19) = 13.13$, $P = 0.002$, $\eta p^2 > 0.41$; component 2, $F(1,19) = 15.13$, $P = 0.001$, $\eta p^2 > 0.44$) but no effect of task (component 1, $F(2,38) = 1.57$, $P = 0.22$; component 2, $F(2,38) = 1.36$, $P = 0.87$) and no task × condition interaction (component 1, $F(2,38) = 1.98$, $P = 0.15$; component 2, $F(2,38) = 0.94$, $P = 0.40$). Activation was also found to be significantly positive compared with zero across all conditions (all ts > 3.81, ps < 0.002, ds > 1.38).

Responses within component 3 resembled those of mid-PGp DMN in the task data. There was a significant effect of violation ($F(1,19) = 10.10$, $P = 0.005$, $\eta p^2 > 0.35$) but no effect of task ($F(2,38) = 2.76$, $P = 0.08$) and no task × condition interaction ($F(2,38) = 0.142$, $P = 0.87$). Responses tended to be negative relative to zero (all ts > 2.53, ps < 0.01, ds > 0.57) except for the picture violation and sentence violation conditions which did not differ from zero ($t < 1.81$, $P > 0.09$).

The response within components 4 and 5 resembled the task-specific responses found for the language network and visual–parietal network from the task data, respectively. Specifically, for component 4 there was a significant effect of task ($F(2,38) = 22.54$,

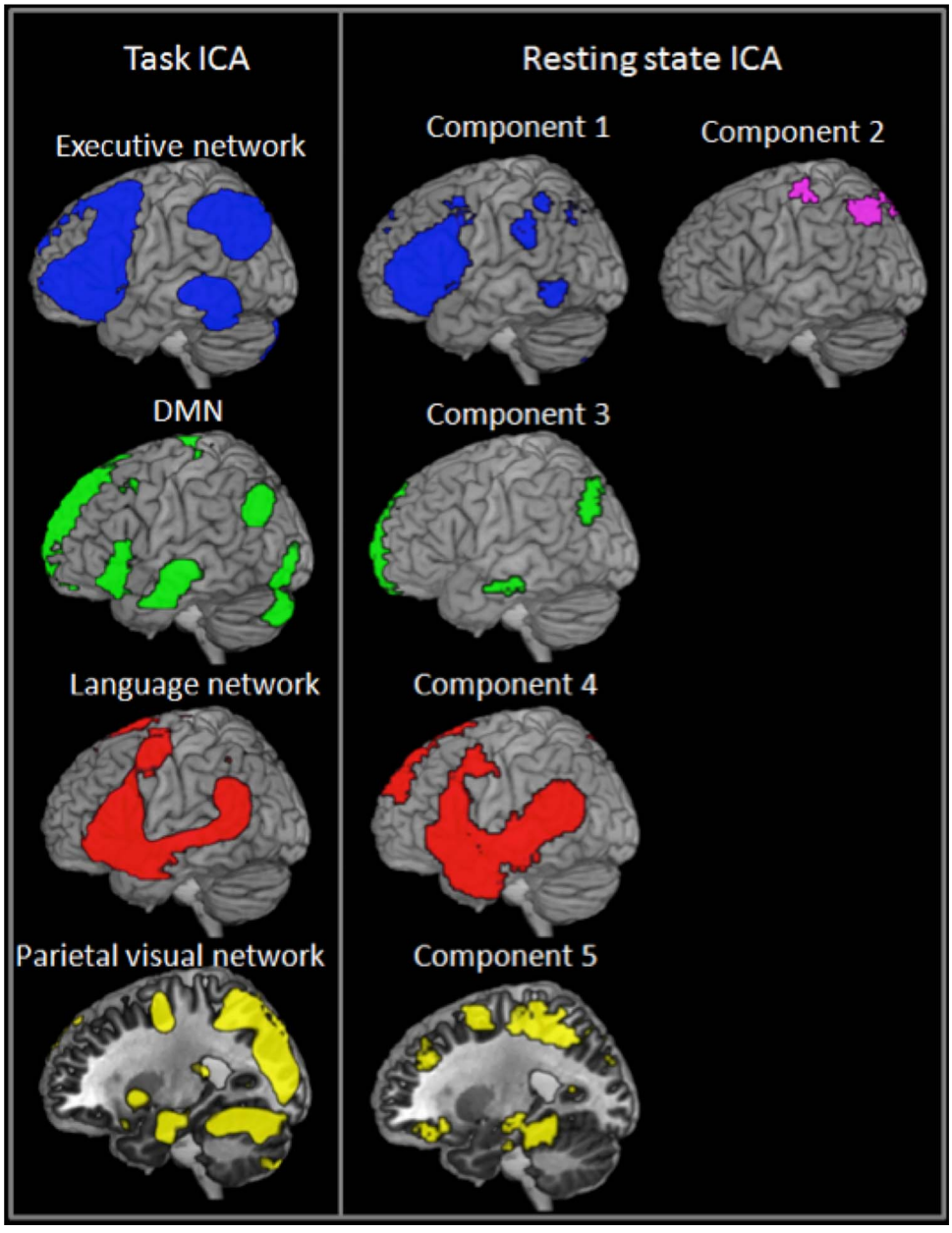

Figure 5. The correspondence between the task ICA and resting state ICA analyses.

$P = 0.001$, $\eta p^2 > 0.67$), violation ($F(1,19) = 7.67$, $P = 0.01$, $\eta p^2 > 0.29$), and a significant task × violation interaction ($F(2,38) = 4.86$, $P = 0.01$, $\eta p^2 > 0.34$). Paired *t*-tests showed greater activation for the sentence task compared with the number task ($t(19) = 4.97$, $P = 0.001$, $d > 1.11$) and picture task ($t(19) = 5.83$, $P = 0.001$, $d > 1.30$) and greater activation for the number task compared with the picture task ($t(19) = 2.62$, $P = 0.02$, $d > 0.58$). Also, the effect of violation was significantly larger in the sentence task compared with the picture task ($t(19) = 2.97$, $P = 0.008$, $d > 0.66$) or the number task ($t(19) = 2.44$, $P = 0.02$, $d > 0.55$), although this was trending using a Bonferroni correction. Compared with zero, responses were significantly positive or trending for the sentence conditions (all ts > 2.34, ps < 0.03, ds > 0.55), did not differ from zero for the number conditions (all ts < 0.34, $P > 0.74$), and were negative for the picture conditions (all ts > 2.52, $P < 0.02$, ds > 0.57).

For component 5, there was a significant effect of violation ($F(1,19) = 19.83$, $P = 0.001$, $\eta p^2 > 0.51$) and task ($F(2,38) = 57.46$, $P = 0.001$, $\eta p^2 > 0.82$) but no task × condition interaction ($F(2,38) = 0.60$, $P = 0.55$). Paired *t*-tests showed that the picture task elicited significantly greater activation compared with the sentence task ($t(19) = 8.09$, $P = 0.001$, $d > 1.81$) and the number task ($t(19) = 8.95$, $P = 0.001$, $d > 2.00$), which did not differ ($t(19) = 0.93$, $P = 0.37$). Against zero, activation was positive for the picture condition (all ts > 4.70, ps < 0.001, ds > 1.10), did not differ from zero for the sentence conditions (all ts < 2.1, $P > 0.05$), and was negative or trending for the number condition (all ts > 1.87, $P < 0.08$, ds > 0.42).

Discussion

The multimethod approach used in this study revealed several key findings with regard the function of the IPC. Aligning with the predictions of the PUCC model (see Introduction section), the highly convergent results can be summarized in terms of three contributing factors.

Factor 1: sensitivity to violation—multiple parts of IPC and the whole executive network are sensitive to sequence violation across domains; they respond more strongly to sequences in which the statistical regularity is violated compared with regular sequences. Despite this general property, the IPC has graded functional subdivisions as observed in the task ICA and replicated using the independently defined ROIs from the resting state ICA. Together these ROI analyses plot out two primary axes of IPC organization (described next).

Factor 2: A dorsal–ventral difference was established with more dorsal areas of AG that approach the IPS (dorsal PGa), forming part of the executive network and responding with positive activation to sequences in a domain-general fashion. In contrast, more ventral areas (mid-PGp) form part of the DMN and are deactivated by all tasks (though mid-PGp was the only part of the DMN that was sensitive to sequential violation). Moreover, the executive network and DMN showed anticorrelated time-series. Together these results suggest that activation of the top-down executive network relate to suppression of the DMN.

Factor 3: the final factor to influence the results was an anterior–posterior dimension of organization within ventral IPC. Ventral PGa formed a part of the language network and hence responded specifically to linguistic material (sentences), whereas ventral PGp was part of the visual/SPL network and hence only responded positively to pictorial material. Also the language and visual–parietal networks selectively correlated with the executive network only when their preferred task was performed. This suggests task-dependent dynamic flexibility in the regions in their interaction with the core, multidemand executive network.

The results show that IPC, together with the executive network, responded to task-general sequence violations. The PUCC model proposes that the IPC may form a neuroanatomically graded multimodal buffer, thereby supporting a dynamic representation of the changing internal and external "state of affairs." As a by-product of repeated events, this system will become sensitive to the temporal and spatial regularities (Plaut 2003). Accordingly, sequence violations are more effortful to process and thus elicit greater activation. The current data are consistent with existing studies finding that IPC responds to the regularities of meaningful (words/picture sequences) and meaningless events (motor/visual sequences) (Kuperberg et al. 2003; Tinaz et al. 2006; Melrose et al. 2008; Tinaz et al. 2008; Bubic et al. 2009; Hoenig and Scheef 2009; Gheysen et al. 2010). Indeed, there is a growing body of evidence that IPC forms part of a context-related processing network. For instance, it responds more strongly to images with strong rather than weak contextual associations (Bar et al. 2008), or when subjects remember contextual associates of an item (Fornito et al. 2012), and is sensitive to event occurrence frequency (d'Acremont et al. 2013). Future studies will be able to explore how these increased IPL activations relate to the underlying processes/computations (e.g., prolonged processing, transient reorienting of attention, transient/sustained control mechanism, etc.) and their exact timings. Such investigations may require formal computational models of these processes and descriptions of the resultant temporally varying neural signatures.

IPC responses were found to be task-general with some variations around the anterior and posterior edges. This supports the notion that there is a core underlying IPC neurocomputation which is common across tasks (Walsh 2003; Cabeza et al. 2012; Humphreys and Lambon Ralph 2015) and argues against a highly "fractionated" or modular pattern of organization (Nelson et al. 2012). Indeed, the current data appear inconsistent with any domain-specific theories of IPC function which, for example, suggest specialization for semantic memory (Geschwind 1972; Binder et al. 2009), episodic memory (Wagner et al. 2005; Vilberg and Rugg 2008; Shimamura 2011), or numerical processing (Arsalidou and Taylor 2011). We consider briefly how each domain-specific theory might address the results of this and other studies. In doing so, we note that these authors might not have intended their theory to provide explanations for data from other cognitive domains, as each theory typically focusses on the primary domain of interest. Most IPC semantic models would predict stronger activation for words and pictures compared with numbers and (presumably) positive activation over and above "rest." The current data clearly do not support this prediction. With regard to episodic-related proposals, there is some convincing evidence that the mid-PGp region is often positively engaged during episodic fMRI tasks (Humphreys and Lambon Ralph 2015) and also shows structural and functional connectivity with other parts of the episodic network including precuneus and hippocampus (Uddin et al. 2010). The experimental manipulation used in the current experiment places limited demands on episodic memory retrieval. Since the task does not require episodic retrieval, this could perhaps explain the consistent deactivation of PGp across domains since the region is not required for this cognitive activity. Nevertheless, any proposal suggesting that the IPC only supports episodic functions could not account for the overall pattern of activation found in the current study, for instance, the anterior–posterior or the dorsal–ventral gradient. Finally, with regard to attention theories of IPC function, direct comparisons between the attention-reorienting literature and those that relate to the DMN and the current paradigm have shown that attentional reorientation is associated with responses within the TPJ (and saliency network), which is anterior to the AG and does not overlap with the current areas of interest (Humphreys and Lambon Ralph 2015). Indeed, the TPJ (and wider saliency network) was found to be entirely insensitive to any manipulation in the current study. Nevertheless, while the posterior IPL is not typically implicated in attention-reorienting functions, one cannot entirely exclude the possibility that the key differences between the current and previous studies might have caused a posterior shift of reorienting-related activity. If this hypothesis is correct, then one must consider what function "triggers" the reorienting mechanism. Indeed, in the current context, the reorienting mechanism must be triggered from a signal derived during sequential processing, which would necessitate a form of temporal buffering, such as that proposed here. Overall, together with previous crossdomain explorations of IPC function (Cabeza et al. 2012; Humphreys et al. 2015; Humphreys and Lambon Ralph 2015, 2017), the current data are more consistent with the notion of a domain-general process but with graded differences in function based on variations in connectivity to different AG subregions.

The ventral PC is involved in bottom-up/stimulus-driven and automatic task components (Cabeza et al. 2012; Humphreys and Lambon Ralph 2015). For instance, AG shows stronger activation

for faster reaction times (Hahn et al. 2007) and is sensitive to a range of tasks with more automated tasks compared with executively demanding tasks, for example, numerical fact retrieval versus numerical calculation, or making semantic decisions on concrete versus abstract words (Humphreys and Lambon Ralph 2015). In contrast, the executive network including dorsal IPC subregions (including dorsal AG and IPS) is known to be involved in top-down processing, responding more strongly to difficult decisions or task demands across diverse domains and task types (Fedorenko et al. 2013; Noonan et al. 2013; Humphreys and Lambon Ralph 2017). The relationship between the bottom-up and top-down networks is unclear, but it is possible that when currently buffered information cannot be automatically processed by the ventral IPC subregions and their connected networks (as in the case of sequence violations), then this triggers the involvement of top-down executive processing systems (see Humphreys and Lambon Ralph 2015 for further discussion). Indeed, this is akin to the notion of a "circuit breaker" proposed by Corbetta and Shulman (2002) in which the stimulus-driven network acts as an alerting system for top-down processing.

Two anatomical gradients of organization were identified within IPC: dorsal–ventral and anterior–posterior. The fact that dorsal (IPS/SPL) and ventral parietal (AG/SMG) areas are functionally dissociable has been recognized by several models of parietal function (Corbetta and Shulman 2002; Cabeza et al. 2008; Humphreys and Lambon Ralph 2015). Indeed, dorsal and ventral PC connect with distinct cortical areas: Central AG forms part of the DMN, whereas IPS/SPL is part of a fronto-parietal control system (Vincent et al. 2008; Spreng et al. 2010; Uddin et al. 2010; Cloutman et al. 2013; Power and Petersen 2013). fMRI studies have also shown that dorsal IPC is associated with task-positive activation, whereas ventral IPC is typically associated with task-negative activation (Fox et al. 2005). The current findings demonstrate that, rather than a sharp dissociation between dorsal (IPS/SPL) and ventral (AG/SMG) areas, there is a graded shift in activation even within the AG: Regions toward IPS become positively activated and relate more strongly to the executive network compared with the DMN. The current results are consistent with a similar graded shift from negative to positive activation in AG observed for semantic tasks (Seghier et al. 2010), though the current study shows that this pattern is not specific to semantic tasks but rather a task-general feature.

The results also showed that the executive network and DMN had anticorrelated time-series. Likewise, resting state studies have frequently shown that these networks are anticorrelated (Fox et al. 2005; Hampson et al. 2010); nevertheless there is evidence to show this dynamic interplay during task performance (Sestieri et al. 2010; Spreng et al. 2010). Future studies are needed to answer the subsequent questions that arise from this repeated observation (see also Humphreys and Lambon Ralph 2015). First, why are any brain regions deactivated at all? Two important possibilities include the observation that rest is not a neutral condition but rather allows in-scanner spontaneous cognition and internal processes and thus "deactivation" might reflect the fact that some active fMRI tasks do not share these cognitive processes (Buckner and Carroll 2007; Raichle and Snyder 2007; Binder et al. 2009; Andrews-Hanna 2012). Another possibility relates to the fact that regions tuned to task-irrelevant functions might be deactivated to save metabolic energy (Attwell and Laughlin 2001; Humphreys et al. 2015). This second possibility is consistent with the results found here for the anterior–posterior changes in function across the ventral IPC (and other findings, see Humphreys and Lambon Ralph 2017). Ventral PGa is tuned more toward language, while ventral PGp for visual tasks. When the active task matches their function, then these regions exhibit positive activation, whereas during other types of tasks, they actually deactivate.

A second puzzle is why the executive and DMN are often (though not always) anticorrelated, with the degree of DMN deactivation and executive network activation both correlated with task/item difficulty, regardless of task (Fedorenko et al. 2013; Humphreys and Lambon Ralph 2017). The PUCC model suggests that the two networks are often counterpointed because ventral IPC buffering for automatic activities, by definition, does not require working memory or "problem-solving" mechanisms, whereas when an ongoing task becomes problematic, the executive network is engaged and ongoing automatic buffering may be counterproductive for problem-solving and thus the buffering is temporarily suspended or suppressed. These notions are similar to previous suggestions for a "safety break" mechanism formed through the dynamic interplay between IPS and IPC and triggered when an unexpected event or stimulus is encountered in the ventral network (Corbetta and Shulman 2002).

The third question relates to what types of task generate task-positive activation in ventral IPC regions and by extension the DMN. These regions are most often associated with task-related deactivation, and thus, understanding the conditions under which task-positive responses are observed might provide critical clues about these regions' core function. This study and related investigations (e.g., Humphreys and Lambon Ralph 2017) provide the first evidence for modality-related variations of processing within AG, which is frequently considered as a modality-general processing area (Binder and Desai 2011) and align with recent proposals that the DMN, more generally, is a multifaceted entity which fractionates depending on the nature of the task that is compared with rest (Buckner et al. 2008; Humphreys et al. 2015; Axelrod et al. 2017). The current study observed this type of fractionation along the ventral IPC region (see also Humphreys et al. 2017): Ventral PGa exhibited deactivation in all conditions except for the language sequences when it was positively activated; ventral PGp showed exactly the reverse pattern. Such results run counter to any single cause or domain-general reason for deactivation but are consistent with notions that areas unnecessary for the current task are deactivated, perhaps to minimize cognitive interference and/or to save metabolic energy (Attwell and Laughlin 2001; Humphreys et al. 2015; Humphreys and Lambon Ralph 2015). The mid-AG remains something of a mystery in that it deactivated across all conditions (albeit being sensitive to sequence violations like the entire IPC region) and is one of the areas consistently associated with the DMN (Buckner et al. 2008). Future crossdomain comparative fMRI studies are required to establish which subtypes of task generate positive activations in the mid-AG and whether these tasks are selective to this IPC subregion, as ventral PGa and PGp appear to be for language and visual tasks, respectively. Possibilities include mind-wandering or other forms of internally directed cognition (Andrews-Hanna 2012), vivid episodic/autobiographical recall (Wagner et al. 2005; Vilberg and Rugg 2008), or future thinking (Buckner and Carroll 2007).

The final question to be considered here pertains to what drives these graded anterior–posterior and superior–ventral graded functional variations across the IPC region? The PUCC model, like other proposals (Cabeza et al. 2012), assumes that, while the IPC might have a core basic neurocomputation (e.g., buffering of current information), subregions come to exhibit

gradedly different responses depending on their pattern of long-range connectivity. This computational principle has been demonstrated previously for PDP models of semantic representation (Plaut 2002). In terms of the anterior–posterior AG gradient, ventral PGa responded positively to the sentence task presumably due to input from the verbally related posterior temporal (STS/MTG) areas, whereas ventral PGp exhibited activation for the picture task, perhaps reflecting greater connectivity to visually related occipital/occipitoparietal regions (Ruschel et al. 2014). In a similar vein, the strong dorsal–ventral IPC variation is likely to reflect differential connectivity, with stronger connections from dorsal AG/IPS regions to DLPFC, thus forming the foundation for the multidemand, executive network (Uddin et al. 2010; Yeo et al. 2011).

To conclude, the IPC exhibits crossdomain sensitivity to sequence violation, consistent with a multimodal buffering computation. This generalized function is conditioned across dorsal–ventral and anterior–posterior dimensions in keeping with variations in long-range connectivity.

Supplementary Material

Supplementary material can be found at *Cerebral Cortex* online.

Notes

This research was supported by an MRC Programme grant to M.A.L.R. (MR/R023883/1), a British Academy fellowship to R.L.J (pf170068), and MRC intramural funding (MC_UU_00005/18).

References

Andrews-Hanna JR. 2012. The brain's default network and its adaptive role in internal mentation. *Neuroscientist*. 18:251–270.

Arsalidou M, Taylor MJ. 2011. Is 2+2=4? Meta-analyses of brain areas needed for numbers and calculations. *Neuroimage*. 54:2382–2393.

Ashburner J. 2007. A fast diffeomorphic image registration algorithm. *Neuroimage*. 38:95–113.

Attwell D, Laughlin SB. 2001. An energy budget for signaling in the grey matter of the brain. *J Cereb Blood Flow Metab*. 21:1133–1145.

Axelrod V, Rees G, Bar M. 2017. The default network and the combination of cognitive processes that mediate self-generated thought. *Nat Hum Behav*. 1:896–910.

Baddeley A. 2003. Working memory: looking back and looking forward. *Nat Rev Neurosci*. 4:829–839.

Bar M, Aminoff E, Schacter DL. 2008. Scenes unseen: the parahippocampal cortex intrinsically subserves contextual associations, not scenes or places per se. *J Neurosci*. 28:8539–8544.

Bell AJ, Sejnowski TJ. 1995. An information-maximization approach to blind separation and blind deconvolution. *Neural Comput*. 7:1129–1159.

Binder JR, Desai RH. 2011. The neurobiology of semantic memory. *Trends Cogn Sci*. 15:527–536.

Binder JR, Desai RH, Graves WW, Conant LL. 2009. Where is the semantic system? A critical review and meta-analysis of 120 functional neuroimaging studies. *Cereb Cortex*. 19:2767–2796.

Block CK, Baldwin CL. 2010. Cloze probability and completion norms for 498 sentences: behavioral and neural validation using event-related potentials. *Behav Res Meth*. 42:665–670.

Bornkessel-Schlesewsky I, Schlesewsky M. 2013. Reconciling time, space and function: a new dorsal-ventral stream model of sentence comprehension. *Brain Lang*. 125:60–76.

Botvinick MM, Plaut DC. 2004. Doing without schema hierarchies: a recurrent connectionist approach to normal and impaired routine sequential action. *Psychol Rev*. 111:395–429.

Botvinick MM, Plaut DC. 2006. Short-term memory for serial order: a recurrent neural network model. *Psychol Rev*. 113:201–233.

Bubic A, von Cramon DY, Jacobsen T, Schroger E, Schubotz RI. 2009. Violation of expectation: neural correlates reflect bases of prediction. *J Cogn Neurosci*. 21:155–168.

Buckner RL, Andrews-Hanna JR, Schacter DL. 2008. The brain's default network—anatomy, function, and relevance to disease. *Ann N Y Acad Sci*. 1124:1–38.

Buckner RL, Carroll DC. 2007. Self-projection and the brain. *Trends Cogn Sci*. 11:49–57.

Buzsaki G, Moser EI. 2013. Memory, navigation and theta rhythm in the hippocampal-entorhinal system. *Nat Neurosci*. 16:130–138.

Bzdok D, Langer M, Schillbach L, Jakobs O, Roski C, Caspers S, Laird AR, Fox PT, Zilles K, Eickhoff SB. 2013. Characterization of the temporo-parietal junction by combining data-driven parcellation, complementary connectivity analyses, and functional decoding. *Neuroimage*. 81:381–392.

Cabeza R, Ciaramelli E, Moscovitch M. 2012. Cognitive contributions of the ventral parietal cortex: an integrative theoretical account. *Trends Cogn Sci*. 16:338–352.

Cabeza R, Ciaramelli E, Olson IR, Moscovitch M. 2008. The parietal cortex and episodic memory: an attentional account. *Nat Rev Neurosci*. 9:613–625.

Calhoun VD, Adali T, Pearlson GD, Pekar JJ. 2001. A method for making group inferences from functional MRI data using independent component analysis. *Hum Brain Mapp*. 14:140–151.

Caspers S, Eickhoff SB, Rick T, von Kapri A, Kuhlen T, Huang R, Shah NJ, Zilles K. 2011. Probabilistic fibre tract analysis of cytoarchitectonically defined human inferior parietal lobule areas reveals similarities to macaques. *Neuroimage*. 58:362–380.

Chao-Gan Y, Yu-Feng Z. 2010. DPARSF: a MATLAB toolbox for "pipeline" data analysis of resting-state fMRI. *Front Syst Neurosci*. 4:13.

Ciaramelli E, Grady CL, Moscovitch M. 2008. Top-down and bottom-up attention to memory: a hypothesis (AtoM) on the role of the posterior parietal cortex in memory retrieval. *Neuropsychologia*. 46:1828–1851.

Cloutman LL, Binney RJ, Morris DM, Parker GJM, Lambon Ralph MA. 2013. Using in vivo probabilistic tractography to reveal two segregated dorsal 'language-cognitive' pathways in the human brain. *Brain Lang*. 127:230–240.

Corbetta M, Shulman GL. 2002. Control of goal-directed and stimulus-driven attention in the brain. *Nat Rev Neurosci*. 3:201–215.

d'Acremont M, Schultz W, Bossaerts P. 2013. The human brain encodes event frequencies while forming subjective beliefs. *J Neurosci*. 33:10887–10897.

Daselaar SM, Huijbers W, Eklund K, Moscovitch M, Cabeza R. 2013. Resting-state functional connectivity of ventral parietal regions associated with attention reorienting and episodic recollection. *Front Hum Neurosci*. 7.

Dehaene S, Piazza M, Pinel P, Cohen L. 2003. Three parietal circuits for number processing. *Cogn Neuropsychol*. 20:487–506.

Fedorenko E, Duncan J, Kanwisher N. 2013. Broad domain generality in focal regions of frontal and parietal cortex. *Proc Natl Acad Sci U S A*. 110:16616–16621.

Fornito A, Harrison BJ, Zalesky A, Simons JS. 2012. Competitive and cooperative dynamics of large-scale brain functional networks supporting recollection. *Proc Natl Acad Sci U S A*. 109:12788–12793.

Fox MD, Snyder AZ, Vincent JL, Corbetta M, Van Essen DC, Raichle ME. 2005. The human brain is intrinsically organized into dynamic, anticorrelated functional networks. *Proc Natl Acad Sci U S A*. 102:9673–9678.

Friston KJ, Williams S, Howard R, Frackowiak RS, Turner R. 1996. Movement-related effects in fMRI time-series. *Magn Reson Med*. 35:346–355.

Geschwind N. 1972. Language and brain. *Sci Am*. 226:–76.

Gheysen F, Van Opstal F, Roggeman C, Van Waelvelde H, Fias W. 2010. Hippocampal contribution to early and later stages of implicit motor sequence learning. *Exp Brain Res*. 202:795–807.

Hahn B, Ross TJ, Stein EA. 2007. Cingulate activation increases dynamically with response speed under stimulus unpredictability. *Cereb Cortex*. 17:1664–1671.

Halai AD, Welbourne SR, Embleton K, Parkes LM. 2014. A comparison of dual gradient-echo and spin-echo fMRI of the inferior temporal lobe. *Hum Brain Mapp*. 35:4118–4128.

Hampson M, Driesen N, Roth JK, Gore JC, Constable RT. 2010. Functional connectivity between task-positive and task-negative brain areas and its relation to working memory performance. *Magn Reson Imaging*. 28:1051–1057.

Hasson U, Yang E, Vallines I, Heeger DJ, Rubin N. 2008. A hierarchy of temporal receptive windows in human cortex. *J Neurosci*. 28:2539–2550.

Hickok G, Poeppel D. 2007. The cortical organization of speech processing. *Nat Rev Neurosci*. 8:393–402.

Hoenig K, Scheef L. 2009. Neural correlates of semantic ambiguity processing during context verification. *Neuroimage*. 45:1009–1019.

Humphreys GF, Hoffman P, Visser M, Binney RJ, Ralph MAL. 2015. Establishing task- and modality-dependent dissociations between the semantic and default mode networks. *Proc Natl Acad Sci U S A*. 112:7857–7862.

Humphreys GF, Lambon Ralph MA. 2015. Fusion and fission of cognitive functions in the human parietal cortex. *Cereb Cortex*. 25:3547–3560.

Humphreys GF, Lambon Ralph MA. 2017. Mapping domain-selective and counterpointed domain-general higher cognitive functions in the lateral parietal cortex: evidence from fMRI comparisons of difficulty-varying semantic versus visuo-spatial tasks, and functional connectivity analyses. *Cereb Cortex*. 27:4199–4212.

Kravitz DJ, Saleem KS, Baker CI, Mishkin M. 2011. A new neural framework for visuospatial processing. *Nat Rev Neurosci*. 12:217–230.

Kuperberg GR, Holcomb PJ, Sitnikova T, Greve D, Dale AM, Caplan D. 2003. Distinct patterns of neural modulation during the processing of conceptual and syntactic anomalies. *J Cogn Neurosci*. 15:272–293.

Lambon Ralph MA. 2014. Neurocognitive insights on conceptual knowledge and its breakdown. *Philos T R Soc B*. 369:1–11.

Lambon Ralph MA, Sage K, Jones RW, Mayberry EJ. 2010. Coherent concepts are computed in the anterior temporal lobes. *Proc Natl Acad Sci U S A*. 107:2717–2722.

Lee MH, Hacker CD, Snyder AZ, Corbetta M, Zhang D, Leuthardt EC, Shimony JS. 2012. Clustering of resting state networks. *PloS One*. 7:e40370.

Leech R, Kamourieh S, Beckmann CF, Sharp DJ. 2011. Fractionating the default mode network: distinct contributions of the ventral and dorsal posterior cingulate cortex to cognitive control. *J Neurosci*. 31:3217–3224.

Lerner Y, Honey CJ, Silbert LJ, Hasson U. 2011. Topographic mapping of a hierarchy of temporal receptive windows using a narrated story. *J Neurosci*. 31:2906–2915.

McClelland JL, John MS, Taraban R. 1989. Sentence comprehension: a parallel distributed processing approach. *Lang Cognit Process*. 4:287–335.

McKeown MJ, Hansen LK, Sejnowski TJ. 2003. Independent component analysis of functional MRI: what is signal and what is noise? *Curr Opin Neurobiol*. 13:620–629.

Melrose RJ, Tinaz S, Castelo JM, Courtney MG, Stern CE. 2008. Compromised fronto-striatal functioning in HIV: an fMRI investigation of semantic event sequencing. *Behav Brain Res*. 188:337–347.

Nelson SM, McDermott KB, Petersen SE. 2012. In favor of a 'fractionation' view of ventral parietal cortex: comment on Cabeza et al. *Trends Cogn Sci*. 16:399–400 author reply 400-391.

Noonan KA, Jefferies E, Visser M, Lambon Ralph MA. 2013. Going beyond inferior prefrontal involvement in semantic control: evidence for the additional contribution of dorsal angular gyrus and posterior middle temporal cortex. *J Cogn Neurosci*. 25:1824–1850.

Plaut DC. 2002. Graded modality-specific specialization in semantics: a computational account of optic aphasia. *Cogn Neuropsychol*. 19:603–639.

Power JD, Cohen AL, Nelson SM, Wig GS, Barnes KA, Church JA, Vogel AC, Laumann TO, Miezin FM, Schlaggar BL *et al*. 2011. Functional network organization of the human brain. *Neuron*. 72:665–678.

Power JD, Mitra A, Laumann TO, Snyder AZ, Schlaggar BL, Petersen SE. 2014. Methods to detect, characterize, and remove motion artifact in resting state fMRI. *Neuroimage*. 84:320–341.

Power JD, Petersen SE. 2013. Control-related systems in the human brain. *Curr Opin Neurobiol*. 23:223–228.

Raichle ME, Snyder AZ. 2007. A default mode of brain function: a brief history of an evolving idea. *Neuroimage*. 37:1083–1090 discussion 1097–1089.

Rauschecker JP, Scott SK. 2009. Maps and streams in the auditory cortex: nonhuman primates illuminate human speech processing. *Nat Neurosci*. 12:718–724.

Robinson SD, Schopf V, Cardoso P, Geissler A, Fischmeister FP, Wurnig M, Trattnig S, Beisteiner R. 2013. Applying independent component analysis to clinical FMRI at 7 t. *Front Hum Neurosci*. 7:496.

Ruschel M, Knosche TR, Friederici AD, Turner R, Geyer S, Anwander A. 2014. Connectivity architecture and subdivision of the human inferior parietal cortex revealed by diffusion MRI. *Cereb Cortex*. 24:2436–2448.

Satterthwaite TD, Elliott MA, Gerraty RT, Ruparel K, Loughead J, Calkins ME, Eickhoff SB, Hakonarson H, Gur RC, Gur RE *et al*. 2013. An improved framework for confound regression and filtering for control of motion artifact in the preprocessing of resting-state functional connectivity data. *Neuroimage*. 64:240–256.

Seghier ML, Fagan E, Price C. 2010. Functional subdivisions in the left angular gyrus where the semantic system meets and diverges from the default network. *J Neurosci*. 30:16809–16817.

Sestieri C, Shulman GL, Corbetta M. 2010. Attention to memory and the environment: functional specialization and dynamic competition in human posterior parietal cortex. *J Neurosci*. 30:8445–8456.

Shimamura AP. 2011. Episodic retrieval and the cortical binding of relational activity. *Cogn Affect Behav Neurosci*. 11:277–291.

Simon O, Mangin JF, Cohen L, Le Bihan D, Dehaene S. 2002. Topographical layout of hand, eye, calculation, and language-related areas in the human parietal lobe. *Neuron*. 33: 475–487.

Spreng RN, Stevens WD, Chamberlain JP, Gilmore AW, Schacter DL. 2010. Default network activity, coupled with the frontoparietal control network, supports goal-directed cognition. *Neuroimage*. 53:303–317.

Stevens MC, Calhoun VD, Kiehl KA. 2005. fMRI in an oddball task: effects of target-to-target interval. *Psychophysiology*. 42:636–642.

Tinaz S, Schendan HE, Schon K, Stern CE. 2006. Evidence for the importance of basal ganglia output nuclei in semantic event sequencing: an fMRI study. *Brain Res*. 1067:239–249.

Tinaz S, Schendan HE, Stern CE. 2008. Fronto-striatal deficit in Parkinson's disease during semantic event sequencing. *Neurobiol Aging*. 29:397–407.

Uddin LQ, Supekar K, Amin H, Rykhlevskaia E, Nguyen DA, Greicius MD, Menon V. 2010. Dissociable connectivity within human angular gyrus and intraparietal sulcus: evidence from functional and structural connectivity. *Cereb Cortex*. 20:2636–2646.

Ueno T, Saito S, Rogers TT, Lambon Ralph MA. 2011. Lichtheim 2: synthesizing aphasia and the neural basis of language in a neurocomputational model of the dual dorsal-ventral language pathways. *Neuron*. 72:385–396.

van der Linden M, Berkers RMWJ, Morris RGM, Fernández G. 2017. Angular gyrus involvement at encoding and retrieval is associated with durable but less specific memories. *J Neurosci*. 37:3603–3616. doi: 10.1523/JNEUROSCI.3603-16.2017.

Van Dijk KR, Sabuncu MR, Buckner RL. 2012. The influence of head motion on intrinsic functional connectivity MRI. *Neuroimage*. 59:431–438.

Vigneau M, Beaucousin V, Herve PY, Duffau H, Crivello F, Houde O, Mazoyer B, Tzourio-Mazoyer N. 2006. Meta-analyzing left hemisphere language areas: phonology, semantics, and sentence processing. *Neuroimage*. 30:1414–1432.

Vilberg KL, Rugg MD. 2008. Memory retrieval and the parietal cortex: a review of evidence from a dual-process perspective. *Neuropsychologia*. 46:1787–1799.

Vincent JL, Kahn I, Snyder AZ, Raichle ME, Buckner RL. 2008. Evidence for a frontoparietal control system revealed by intrinsic functional connectivity. *J Neurophysiol*. 100:3328–3342.

Wagner AD, Shannon BJ, Kahn I, Buckner RL. 2005. Parietal lobe contributions to episodic memory retrieval. *Trends Cogn Sci*. 9:445–453.

Walsh V. 2003. A theory of magnitude: common cortical metrics of time, space and quantity. *Trends Cogn Sci*. 7:483–488.

Weissenbacher A, Kasess C, Gerstl F, Lanzenberger R, Moser E, Windischberger C. 2009. Correlations and anticorrelations in resting-state functional connectivity MRI: a quantitative comparison of preprocessing strategies. *Neuroimage*. 47:1408–1416.

Xu J, Potenza M, Calhoun VD. 2013. Spatial ICA reveals functional activity hidden from traditional fMRI GLM-based analyses. *Front Neurosci*. 7:154.

Xu J, Potenza M, Calhoun VD, Zhang R, Yip SW, Wall JT, Pearlson GD, Worhunsky PD, Garrison KA, Moran JM. 2016. Large-scale functional network overlap is a general property of brain functional organization: reconciling inconsistent fMRI findings from general-linear-model-based analyses. *Neurosci Biobehav Rev*. 71:83–100.

Yan CG, Cheung B, Kelly C, Colcombe S, Craddock RC, Di Martino A, Li Q, Zuo XN, Castellanos FX, Milham MP. 2013. A comprehensive assessment of regional variation in the impact of head micromovements on functional connectomics. *Neuroimage*. 76:183–201.

Yeo BT, Krienen FM, Chee MW, Buckner RL. 2013. Estimates of segregation and overlap of functional connectivity networks in the human cerebral cortex. *Neuroimage*. 88C:212–227.

Yeo BT, Krienen FM, Sepulcre J, Sabuncu MR, Lashkari D, Hollinshead M, Roffman JL, Smoller JW, Zoller L, Polimeni JR *et al*. 2011. The organization of the human cerebral cortex estimated by intrinsic functional connectivity. *J Neurophysiol*. 106:1125–1165.